Cellular defense processes regulated by pathogen-elicited receptor signaling

Citation: Wu, Rongcong, Arthur Goldsipe, David B. Schauer, and Douglas A. Lauffenburger. "Cellular Defense Processes Regulated by Pathogen-Elicited Receptor Signaling." Edited by Harold Szu. Independent Component Analyses, Wavelets, Neural Networks, Biosystems, and Nanoengineering IX (May 13, 2011). © Society of Photo-Optical Instrumentation Engineers (SPIE)

As Published: http://dx.doi.org/10.1117/12.889123

Publisher: SPIE

Persistent URL: http://hdl.handle.net/1721.1/88972

Version: Final published version: final published article, as it appeared in a journal, conference proceedings, or other formally published context

Cellular defense processes regulated by pathogen-elicited receptor signaling

Rongcong Wu, Arthur Goldsipe, David B. Schauer, Douglas A. Lauffenburger
Department of Biological Engineering,
Massachusetts Institute of Technology,
Cambridge MA 02139
10th April 2011

ABSTRACT

Vertebrates are constantly threatened by the invasion of microorganisms and have evolved systems of immunity to eliminate infectious pathogens in the body. Initial sensing of microbial agents is mediated by the recognition of pathogens by means of molecular structures expressed uniquely by microbes of a given type. So-called 'Toll-like receptors' are expressed on host epithelial barrier cells play an essential role in the host defense against microbial pathogens by inducing cell responses (e.g., proliferation, death, cytokine secretion) via activation of intracellular signaling networks. As these networks, comprising multiple interconnecting dynamic pathways, represent highly complex multi-variate "information processing" systems, the signaling activities particularly critical for governing the host cell responses are poorly understood and not easily ascertained by *a priori* theoretical notions. We have developed over the past half-decade a "data-driven" computational modeling approach, on a 'cue-signal-response' combined experiment/computation paradigm, to elucidate key multi-variate signaling relationships governing the cell responses. In an example presented here, we study how a canonical set of six kinase pathways combine to effect microbial agent-induced apoptotic death of a macrophage cell line. One modeling technique, partial least-squares regression, yielded the following key insights: {a} signal combinations most strongly correlated to apoptotic death are orthogonal to those most strongly correlated with release of inflammatory cytokines; {b} the ratio of two key pathway activities is the most powerful predictor of microbe-induced macrophage apoptotic death; {c} the most influential time-window of this signaling activity ratio is surprisingly fast: less than one hour after microbe stimulation.

KEYWORDS

Systems biology; cell signaling; computational modeling; pathogen/host interactions; microbial infection

Independent Component Analyses, Wavelets, Neural Networks, Biosystems, and Nanoengineering IX,
edited by Harold Szu, Liyi Dai, Proc. of SPIE Vol. 8058, 80581I · © 2011 SPIE
CCC code: 0277-786X/11/$18 · doi: 10.1117/12.889123

INTRODUCTION

Toll-like receptors (TLRs), a family of type I transmembrane receptors, have been well documented to recognize pathogen-associated molecular patterns (PAMPs) through a highly variable extracellular region containing a leucine-rich repeat (LRR) domain and play an essential role in the host defense against microbial pathogens. To date, more than 11 human TLRs and 13 mouse TLRs have been identified, and their homodimers or heterodimers can recognize a variety of PAMPs ranging from bacterial and viral components to fungal and protozoal molecules [1]. With respect to the focus of our study here, lipopolysaccharide (LPS) that is uniquely expressed in the outer membrane of cell wall by gram-negative bacteria is specifically recognized by TLR-4. Activity of Toll-like receptor-4 (TLR-4) in macrophages is essential in host defense against bacterial infection. By recognition of specific pathogen-associated molecular patterns such as lipopolysaccharide (LPS), TLR-4 concomitantly initiates a set of downstream signaling pathways regulating cytokine release and apoptotic death responses involved in the innate immune response. Especially with respect to apoptosis, although individual pathways have been implicated in influencing macrophage behavior there is little understanding concerning the integrative operation of multiple pathways as a governing network.

Generally, after recognition of PAMPs TLRs activate a cascade of intracellular signaling events through highly conserved TIR homology domains localized in their intracellular tails [2]. TLR-4 recruits two sets of adaptors (MyD88-MAL and TRAM-TRIF), although these adaptors are also shared with other TLRs, and initiates multiple downstream signaling pathways (Figure 1). The MyD88-MAL-dependent pathway recruits IRAK-1 and IRAK-4, which then phosphorylate TRAF-6 leading to the activation of MKK complexes and IKK complex by binding to and activating TAK1. Subsequently, activated MKK complexes and IKK complex phosphorylate several pivotal downstream kinases, including ERK1/2, p38 MAPK, JNK/SAPK and IKKab, which then co-regulate many transcription factors, such as ATF-2, c-Jun, Elk, NF-kB, and so on, to control various cell responses, including pro- or anti-inflammatory cytokine/chemokine release and apoptosis. In contrast, the TRAM-TRIF-dependent pathway recruits and activates TBK1 and IKKe [3], which then phosphorylates IRF-3 to control the transcription of IFN-inducible genes. Moreover, the TRAM-TRIF-dependent pathway also associates with TRAF-6 [4, 5] and RIP1 [2, 5] to crosstalk with the MyD88-MAL-dependent pathway. Additionally, LPS-stimulated activation of PI3K is also observed and might involve TLR-4, although the precise mechanism remains to be determined [6, 7]. The activation of PI3K and its downstream kinase, Akt/PKB is thought to act as a negative regulator of the MyD88-MAL-dependent pathway by inactivating ERK1/2, p38 MAPK, JNK and IKKab through unknown mechanisms [2, 7-9] and probably also by regulating the activity of BTK, which phosphorylates MAL and then interacts with SOCS-1 resulting in MAL polyubiquitination and subsequent degradation [6, 10]. At the same time, autophosphorylation and activation of PKR, which subsequently phosphorylates eIF2a to inhibit protein synthesis, has been well documented [11, 12], but the mechanism leading to PKR activation downstream of LPS stimulation remains obscure.

Besides the above forward cascades, there also exist constitutively expressed or inducible endogenous negative regulators in the TLR-4 signaling network, which target different stages of the pathways with apparent result of ensuring that appropriate responses ensue. These include soluble MyD88s, SOCS1, IRAK-M, TOLLIP, ST2L, A20, SIGIRR, TRAILR, and TRIAD3A, which downregulate adaptors and/or kinases, resulting in turndown of proximal signal transduction of MyD88-MAL-dependent pathways [2]. At the same time, dual-specificity protein phosphatases (DUSPs), also referred to as MAPK phosphatases (MKPs) in mammalian cells, target the mitogen-activated protein kinases (MAPKs), selectively dephosphorylating and inactivatingERK1/2, p38 MAPK and/or JNK. To date more than

10 MKPs have been identified in mammalian cells, but how exactly they are induced and what their substrate specificities are remain questions of active investigation. For instance, although MKP-1 was initially thought to be a specific phosphatase of ERK1/2, emerging evidences indicates that MKP-1 can inactivate p38 MAPK and JNK preferentially [13, 14]. Induction of MKP-1 was recently demonstrated to be controlled by p38 MAPK and MK2 [15], although some groups argue that ERK1/2 is more important in this process [13, 15].

In addition to the more intensely studied cytokine release behavior of macrophages, apoptotic death plays a crucial role in certain pathogenic infections [16]. The strategies applied by microbes to activate or inhibit apoptosis are probably necessary to subvert normal host defense responses to protect them from being cleared from the host [16, 17]. A number of pathogens have been reported to exhibit an array of virulence determinants that interact with key components of cell death pathways of the host or interfere with the regulation of transcription factors monitoring cell survival [18]. For example, *Legionella* (including *L. pneumophila* and *L. micdadei*) have been shown to induce apoptosis in macrophages via the activation of caspase-3 independently of *de novo* protein synthesis, and *Legionella*-induced apoptosis was completely blocked by caspase-3 inhibitors [18]. In contrast, *Yersinia* injects into host cells proteins altering kinase signaling pathway activities [19]. *Yersinia* outer protein YopJ (in *Y. pestis* and *Y. pseudotuberculosis*) or YopP (in *Y. enterocolitica*) inactivate MKKs and IKKb, likely by interfering with ubiquitin-mediated degradation [20, 21], generating swift apoptotic death [19, 22]. Since the inhibition of MKKs by YopJ or YopP can prevent the activation of several downstream MAPKs, including ERK1/2, JNK and p38 MAPK simultaneously [20, 22], the contribution of these kinases to *Yersinia*-induced apoptosis is an issue of significant relevance. Previous reports have demonstrated that the engagement of TLR-4 and the inhibition of p38 MAPK both are indispensable for *Yersinia*-induced apoptosis [23, 24], motivating use of a relatively specific p38 inhibitor, SB202190, for further study of the roles of other network signals such as IKK, ERK, and JNK.

Clearly, knowledge of the components involved in the TLR-4 signaling network, but how its individual pathway activities work together to determine cell death-versus-survival fate remains murky. This may be at least partially ascribed to the fact that most previous research has focused on how the abnormal performance of an individual component or pathway in the network might perturb cell responses, without explicit consideration of integration and crosstalk. In other systems, quantitative combinations of multiple signals have been typically found necessary in order to effectively predict cell behavioral responses [25-28]. Hence, here we also hypothesize that an intricate working pattern might be exhibited by TLR-4 signaling network in determining its outputs, and sought to obtain some new insights that might be helpful to address the unsolved biological questions and applied to develop new drugs against infectious diseases through systematic analysis and quantitative modeling.

MATERIALS AND METHODS

Cell culture

RAW264.7 cells were purchased from ATCC and grown in Dulbecco's Modified Eagle's Medium (DMEM, Invitrogen) freshly prepared using endotoxin-free water and supplemented with 10% heat-inactivated fetal bovine serum, 1.5 g/l sodium bicarbonate, 100 mg/ml streptomycin and 100 U/ml penicillin. The cultures were maintained at 37 ºC in a humidified 5% CO_2 atmosphere.

LPS

We purchased LPS O55:B5 from Sigma-Aldrich, and repurified it before treating cells. The repurification procedure was dissolution in endotoxin-free water with 0.2% triethylamine (TEA) and 0.5% deoxycholate (DOC), extraction with equal-volume water-saturated phenol, precipitation in 75% ethanol and 30 mM sodium acetate solution at -20ºC for 1 h, and then air-dry at 4ºC after precipitates were washed with cold 100% ethanol. Recovery was almost one hundred percent, and this method has been demonstrated to effectively eliminate signaling through TLR-2 without loss of TLR-4 activation. Finally, we resuspended our phenol re-extracted LPS in endotoxin-free 0.2% TEA at 5 mg/ml stock concentration and stored the aliquots at -20ºC for long-term use (stable up to 2 years) or at 4ºC for up to one month.

Pharmacological agents

The following reagents, unless indicated otherwise, were all purchased from Sigma-Aldrich. SB202190, SB203580, PD980065, U0126 (Calbiochem), wortmannin, LY294002, JNKi VIII (Calbiochem), SP600125 and PS1145 were all dissolved in dimethyl sulfoxide (DMSO), stored at -20 ºC and protected from light. In all experiments, exponentially growing cells were seeded at an initial cell density of $2\times10^5/cm^2$ for the following 24 h of culture and exposed to treatment for the times indicated.

Apoptosis assay

For 7-AAD & Annexin V-PE double staining analysis, we used Annexin V-PE apoptosis detection kit I purchased from BD PharMingen™. For anti-active caspase-3-Alexa 488 & anti-cleaved PARP-Alexa 647 double staining analysis, we purchased primary antibodies, purified rabbit anti-active caspase-3 and purified mouse anti-cleaved PARP (Asp214), from BD PharMingen™ and secondary antibodies, Alexa 488-linked goat anti-rabbit IgG (H+L) and Alexa 647-linked anti-mouse IgG_1 (g1), from Invitrogen™.

Cytokine release assay

In this study, we focused on three inflammatory cytokines commonly appreciated to be secreted by macrophages: IL-6, which plays an important role in triggering the acute phase response of the body to injury or inflammation, IL-12, which mediates enhancement of the cytotoxic activity of NK cells and CD8+ cytotoxic T lymphocytes, and TNF-a, a pleiotropic cytokine that regulates a broad range of biological activities, including cell differentiation, proliferation and death, as well as inflammation, innate and adaptive immune responses, and tissue development. We employed a sandwich ELISA assay, with paired unlabeled and biotinylated antibodies purchased from BD PharMingen™: purified rat anti-mouse IL-6 (clone: MP5-20F3) vs. biotin rat anti-mouse IL-6 (clone: MP5-32C11); purified rat anti-mouse IL-12 p40/p70 (clone: C15.6) vs. Biotin rat anti-mouse IL-12 p40/p70 (clone: C17.8); and, purified hamster ant-mouse/rat TNF (clone: TN3-19.12) vs. biotin rabbit anti-mouse/rat TNF (clone: C1150-14). We used standard curve calibration to quantify absolute amounts of secreted IL-6, IL-12 and TNF-a in the media. The standard curve was generated for each individual plate using serially diluted purified recombinant mouse IL-6, IL-12 or TNF-a of known

concentrations which should encompass the levels in the experimental samples and stay within the linear range.

Western blot assay

We employed western blotting to indirectly monitor the activation of several kinases in TLR-4 signaling network by examining the phosphorylation of serine (Ser), threonine (Thr), and/or tyrosine (Tyr) residuals at their specific sites. The phospho-specific antibodies that we used included anti-phospho-p38 MAPK(Thr180/Tyr182), anti-phospho-JNK(Thr183/ Tyr185), anti-phospho-ERK1/2(Thr202/Tyr204), anti-phospho-MK2(Thr334), anti-phospho-IKKa/b(Ser176/180), anti-phospho-Akt(Ser473), anti-phospho- eIF2a(Ser51), anti-phospho-c-Jun(Ser73), and anti-phospho-ATF-2(Thr69/71), and the phosphorylation of indicated residuals in the parentheses has been demonstrated to be indispensable for full activities of corresponding kinases in response to LPS insults. LPS induced dose-dependent phosphorylation of p38 MAPK, JNK and MK2 and ERK1/2, reaching a plateau after 10 ng/ml. This result strongly supported our hypothesis that saturation of TLR-4 signaling transduction might be achieved and account for the plateaus observed in the measurement of apoptosis and cytokine secretion. In addition, we also examined the effects of SB202190 and/or LPS treatment on the expression of total p38 MAPK and JNK proteins and saw there was no significant change. For quantitative data, we developed a protocol using the Amersham ECLTM advance western blotting detection kit, directly developing and quantitating the blots using Kodak Image Station 1000 with Kodak 1D software instead of burning medical X-ray films in a dark room. We determined linear dynamic ranges by preparing two different standard samples: standard sample 1 (SD1) was the lysate of RAW264.7 cells treated with 1 mg/ml LPS for 30 min and standard sample 2 (SD2) was the lysate of RAW264.7 cells treated with 5 mg/ml tunicamycin from *Streptomyces sp.* for 6 hours. SD2 was utilized to determine the linear range of phospho-eIF2a (Ser51) while SD1 for the others.

Principal Components Analysis and Partial Least-Squares Regression modeling

First, we sought to explore the potential biological significances hiding in each individual data block by clustering their relevant intra-variables through principal component analysis (PCA). PCA is a nondirected multivariate analysis technique that employs singular value decomposition to separate linearly mixed raw data into a structure part and noise part in a block-based manner [29]. The model can be displayed by the following equation: $X = TP^T+E$ (T: scores matrix, P^T: loadings matrix, E: error matrix). The fundamental idea is to use fewer dimensions to replace a complex multidimensional dataset, but still be considered a good approximation to fit the original data closely enough. In particular, the resulting scores matrix and loadings matrix can also help us to find out in what respect one sample is different from another, which variables contribute most to this difference, and whether the variables contribute in the same way or are independent of one another.

Our next step in data analysis focused on attempts to explore the potential relationships between TLR-4 signaling and apoptosis. To attain this aim, we used PLSR, since it is designed to generate data-driven predictive models that relate a matrix, or block, of independent measurements to a block of dependent measurements or classifications. As mentioned previously, our data had been cast in three blocks respectively representing cues, signals and responses. Any one of them can act as independent or dependent blocks in PLSR modeling, but it is conceptually helpful to

organize them according to the cause-effect relationship. Therefore, we set the signal block as the independent block and set the response block as the dependent block. Unlike PCA, which extracts latent variables to maximize the information captured from a single dataset, PLSR executes a simultaneous and interdependent PCA decomposition in both independent (X) and dependent (Y) blocks in such a way that the information in the Y block is used directly as a guide for optimal decomposition of the X block, and subsequently performs regression of Y [30]. The model equation can be written as: $Y = XW^*C^T+F$ ($W^*=W(P^TW)^{-1}$, W: X weights matrix, C^T: Y weights matrix, F: residuals matrix) [31]. Hence, the resulting w^*c vs. w^*c plots can show the correlation structure between X and Y, including how the X and Y variables combine in the projections and how the X variables relate to Y. In addition, three parameters, respectively called $R^2Y(cum)$, $Q^2(cum)$ and ∑DmodY, have been proposed to evaluate the quality of constructed PLSR models [46, 56]. $R^2Y(cum)$ is a measure of how well the model fits the data and a value close to 1 is desired for a good model. $Q^2(cum)$ indicates how well the model predicts new data and a large value (> 0.5) indicates good predictivity. ∑DModY is the distance of the observation in the training set to the Y model plane or hyper plane. No critical limits are shown for ∑DModY, but the smaller value is better. Furthermore, there is also a parameter, called variable importance for the projection (VIP), proposed to evaluate the importance of the variables [31]. VIP values larger than 1 indicate important X variables, and values lower than 0.5 indicate unimportant X variables. A good PLSR model usually is powerful to identify the determinative changes in a particular response, even when the characteristics of many other proteins are varying simultaneously, since it can highlight the measurements that strongly co-vary with the known outcome and deemphasizing those that do not.

RESULTS

Quantitative measurement of cell signaling and phenotypic responses to LPS and p38 inhibitor treatment

As a first step, we developed a landscape of various cue (i.e., treatment) conditions, to probe different facets of cell signaling and response states. Based on this principle, we chose 13 different combinations of LPS and SB202190 to probe our system of RAW264.7 cells: LPS at 0, 0.3, 1, and 5 mg/ml and SB202190 at 0, 10, 50, and 75 mM. All treatments contained the same amounts of vehicle (0.2% TEA and DMSE). As shown in Figure 2, combination of LPS and p38 inhibition lead to enhanced induction of apoptosis. And as shown in Figure 3, LPS concomitantly induced the secretion of both IL-6 and TNFa, with p38 pathway inhibition diminishing this effect.

Figure 4 shows the dynamic profiles of six key kinase signals: JNK, ERK1/2, MK2, Akt, IKKa/b, and eIF2a. These are distributed in relatively independent branched downstream pathways of the TLR-4 signaling network, with aim to provide a useful representation of the signaling network state. It is evident that the profiles of these six phosphorylated kinases are quite different from each other, for both LPS stimulation and p38 inhibition. Thus, we need to seek predictive insights for relating these pathway signals to the apoptosis and cytokine secretion responses.

Computational modeling analysis of signal-response relationships induced by LPS and p38 inhibitor treatment

To do this, we cast our data in three blocks, respectively termed ‘cue’, ‘signal’, and ‘response’. The cue block was a description matrix containing the detailed information of 13 cue treatments, while the signal block and the response block respectively consisted of our compiled phosphorylation measurements (Figure 4) and cell response

measurements (Figures 2 and 3). Since the different time points were collected from separate tissue culture plates, the individual time points from 13 treatments were considered as independent samples for the purpose of the multivariate analysis. Moreover, all the measurements were made on samples prepared under identical conditions, so we can safely include these in the same sample row. Accordingly, the final dimensions of the signal block and the response block were respectively 13 × 42 and 13 × 4 without empty elements.

First, we sought to explore the potential biological significances hiding in each individual data block by clustering their relevant intra-variables through principal component analysis (PCA). PCA is a non-directed multivariate analysis technique that employs singular value decomposition to separate linearly mixed raw data into a structure part and noise part in a block-based manner (see Materials and Methods). As shown in Figure 5, 13 samples or treatments were mapped almost linearly in two distinct directions that respectively represented increasing apoptosis and increasing secretion of IL-6 and TNF-a in scores plot. Interestingly, these two directions appeared to be closely orthogonal, suggesting that the occurrence of these two cell responses was probably independent. In other words, LPS-induced secretion of IL-6 and TNF-a might have no impact on LPS plus SB202190-induced apoptosis through autocrine while the activation of caspase-3 in apoptotic cells might not interfere with the secretion of IL-6 and TNF-a either.

Our next step in data analysis focused on attempts to explore the potential relationships between TLR-4 signaling and apoptosis. To attain this aim, we used PLSR, since it is designed to generate data-driven predictive models that relate a matrix, or block, of independent measurements to a block of dependent measurements or classifications. As mentioned previously, our data had been cast in three blocks respectively representing cues, signals and responses. Any one of them can act as independent or dependent blocks in PLSR modeling, but it is conceptually helpful to organize them according to the cause-effect relationship. Therefore, we set the signal block as the independent block and set the response block as the dependent block. PLSR executes a simultaneous and interdependent PCA decomposition in both independent (X) and dependent (Y) blocks in such a way that the information in the Y block is used directly as a guide for optimal decomposition of the X block, and subsequently performs regression of Y. A good PLSR model usually is powerful to identify the determinative changes in a particular response, even when the characteristics of many other proteins are varying simultaneously, since it can highlight the measurements that strongly co-vary with the known outcome and deemphasizing those that do not.

We constructed a ‘full model’ using the whole signal block, and then also single kinase models using its individual kinase subsets. All single kinase models performed poorly, suggesting that a satisfactory model relating signals downstream of TLR-4 activation to induction of apoptosis in RAW264.7 cells requires a quantitative combination of measurements from multiple pathways. Particularly, we noticed that JNK and ERK1/2 had opposite effects on LPS plus SB202190-induced apoptosis conveyed by the data of SP600125, PD980059 and U0126-treated samples (data not shown). Since some microtubule inhibitors (e.g., Taxol, vinblastine, vincristine, and colchicine) [32] and lipids (e.g., ceramide and sphingosine) [33] induced apoptosis was reported to correlate with the imbalance of JNK and ERK activation, we asked whether the ratio of phosphorylated JNK and ERK1/2 could determine LPS plus SB202190 induced RAW264.7 apoptosis. To test this hypothesis, we subsequently performed PLSR modeling for each possible pair (about 28) of phosphorylated kinases (here ERK1, ERK2 and total ERK were treated as three individual kinases) using datasets consisting of their ratios across all 13 samples and 6 time points. Interestingly, four different kinase ratio PLSR models exhibited both good $R^2Y(cum)$ and $Q^2(cum)$ values (> 0.5) while others exemplified by the JNK2/IKKa/b model performed poorly (Figure 6). In order to ascertain time-relationships associated with these four

kinase-ratio PLSR models, we investigated the effects of the timing of U0126 addition on LPS plus SB202190-induced apoptosis. Our hypothesis was that if apoptosis is determined by the ratio at a specific time point, the addition of U0126 before that time point should promote LPS plus SB202190 induced apoptosis to the similar extent and instead to a smaller extent if apoptosis is initiated after that time point. As shown in Figure 7, such a time point exists in our system and is around 1 hour after LPS addition. Moreover, LPS plus SB202190-induced apoptosis should progress stably as well since apoptosis decreased steadily with the timing increase of U0126 addition. All results were consistent with the prediction of the JNK2/ERK1 and JNK2/ERK models, suggesting that these two models might perform better in presenting TLR-4 signaling-mediated apoptosis though they had a little bit lower $R^2Y(cum)$ and $Q^2(cum)$ values than those of the JNK2/MK2 model.

Experimental test of kinase ratio model predictions

In order to evaluate our constructed PLSR models more convincingly, we sought to undertake a direct a priori experimental prediction of key model predictions using an independent dataset. In order to make our new dataset really independent of the training dataset, we had introduced new interventions to perturb our system; these were the PI3K inhibitor wortmannin, the MEK inhibitor U0126, and the JNK inhibitor SP600125. Altogether, these provided a set of 6 new treatments as listed in the table below, from which new signaling and response data were generated.

Table -- New treatments for model prediction test

Treatments	1	2	3	4	5	6
LPS (ng/ml)	5	1	5	5	5	1
SB202190 (mM)	75	75	75	75	75	75
U0126 (nM)	250	500	—	—	250	500
SP600125 (mM)	—	—	5	10	10	10

Note: All the treatments contained the same amounts of drug vehicles (0.2% TEA and DMSO). DMSO, SB202190, U0126 and SP600125 were added 30 min prior to 0.2% TEA and LPS.

The results of this test are shown in Figure 8. A full model based on all the signals is observed to have far smaller RMSE values than that of the full model built with the control sample excluded, though the latter had a higher $Q^2(cum)$ value. Notwithstanding, both of them performed poorly. That might suggest we had gotten over-fitted models that just represent the pattern of random noise or individual features of the training dataset, and instead other kinases, proteins or pathways that play a critical role in regulation of LPS plus SB202190-induced apoptosis were not involved in our full models. However, when we zoomed in on the full model plot (green rectangle), we found the full model, in fact, predicted U0126-free samples quite well (RMSE = 6.38 and $R^2 = 0.90$), thereby raising another possibility that a nonlinear correlation between kinases and apoptosis might exist in RAW264.7 cells. Actually, all our four kinase-ratio PLSR models exhibited excellent predictivity on these independent datasets, although the JNK2/ERK2 and JNK/MK2

models performed a little bit worse and were likely to underpredict the samples. All these results were consistent with our previous experimental validation, further confirming that TLR-4 signaling mediated apoptosis can be well described and predicted by a simple two-kinase PLSR model, the JNK2/ERK1 model or JNK2/ERK model. In other words, the inhibition of p38 MAPK might regulate LPS-induced apoptosis by simply increasing the ratio of activated JNK and ERK.

DISCUSSION

As an important sensor for bacterial infection, TLR-4 is the most intensively studied member of the TLR family since it was first identified in humans in 1997 [34]. A canonical TLR-4 signaling network (Figure 1) has already been constructed under the contributions of scientists all over the world, though some details still remain controversial and missing, providing the fundamental for us to do systematic analysis of TLR-4 signaling mediated cell responses. Through the measurements of the phosphorylation levels of 6 kinases distributed in different branched downstream pathways of TLR-4 signaling network at 6 time points in response to various combinations of LPS and SB202190 by developed quantitative western blot, we find that the inhibition of p38 MAPK can extend the phosphorylation of several kinases including JNK, ERK1/2 and IKKa/b to different extent, and our PCA models further reveal that such extension will probably alter the activities of these kinases on the timing. In fact, we observed LPS plus SB202190-induced apoptosis was initiated after 1 hour exactly when the phosphorylation of JNK and ERK1/2 was extended. Our results also indirectly highlight that negative feedbacks, such as MKPs [23], in TLR-4 signaling network might regulate cell death as well as cytokine release.

An especially important accomplishment of this study is the successful construction of predictive PLSR models and through these models we have obtained some new insights on TLR-4-signaling mediated cytokine secretion and apoptosis. Besides, we also find that PLSR models built using the ratio of activated JNK2 and ERKs, especially ERK1, can capture the information of apoptosis induced by LPS plus SB202190 well. Unlike the Akt only model, these kinase-ratio models also possess an excellent predictivity on independent datasets, suggesting that LPS plus SB202190 might really trigger apoptosis in RAW264.7 cells through increase of the ratio of activated JNK and ERK. Obviously, these two kinases could be developed as new drug targets to protect the host from being killed by some bacteria, such as *Yersinia* and *Bacillus anthracis*, which can kill macrophages in a manner dependent on the inhibition of p38 MAPK by their virulence determinants (YopP or YopJ and LT) [19, 22]. For example, we might use small molecules to inhibit the activation of JNK or/and promote the activation of ERK through some extracellular signals. Moreover, Since JNK, ERK and p38 MAPK pathways are shared with other TLRs, it might be possible to use this mechanism to selectively and rapidly kill some virus-infected cells in case the activation of p38 MAPK is blocked.

ACKNOWLEGEMENTS

This work was partially supported by the Army Institute for Collaborative Biotechnologies, along with the NIGMS Center for Cell Decision Processes.

REFERENCES

1. Akira S, Uematsu S, and Takeuchi O. Pathogen recognition and innate immunity. *Cell*. 124: 783-801. (2006)

2. Liew FY, Xu D, Brint, EK, and O'Neill LAJ. Negative regulation of Toll-like receptor-mediated immune responses. *Nat. Rev. Immunol.* 5: 446-458. (2005)

3. Sharma S, tenOever BR, Grandvaux N, Zhou GP, Lin R, and Hiscott J. Triggering the interferon antiviral response through an IKK-related pathway. *Science.* 300: 1148-1151. (2003)

4. Sato S, Sugiyama M, Yamamoto M, Watanabe Y, Kawai T, Takeda K, and Akira S. Toll/IL-1 receptor domain-containing adaptor inducing IFN-b (TRIF) associates with TNF receptor-associated factor 6 and TANK-binding kinase 1, and activates two distinct transcription factors, NF-kB and IFN-regulatory factor-3, in the Toll- like receptor signaling. *J. Immunol.* 171: 4304-4310. (2003)

5. Kawai T, and Akira S. TLR signaling. *Cell Death Differ.* 13: 816-825. (2006)

6. Okkenhaug K, and Vanhaesebroeck B. PI3K in lymphocyte development, differentiation and activation. *Nat. Rev. Immunol.* 3: 317-330. (2003)

7. Fukao T, and Koyasu S. PI3K and negative regulation of TLR signaling. *Trends Immunol.* 24(7): 358-363. (2003)

8. Guha M, and Mackman N. The phosphatidylinositol 3-kinase-Akt pathway limits lipopolysaccharide activation of signaling pathways and expression of inflammatory mediators in human monocytic cells. *J. Biol. Chem.* 277(35): 22124-32132. (2002)

9. Ojaniemi M, Glumoff V, Harju K, Liljeroos M, Vuori K, and Hallman M. Phosphatidylinositol 3-kinase is involved in Toll-like receptor-4-mediated cytokine expression in mouse macrophages. *Eur. J. Immunol.* 33: 597-605. (2003)

10. Mansell A, Smith R, Doyle SL, Gray P, Fenner JE, Crack PJ, Nicholson SE, Hilton DJ, O'Neill LAJ, and Hertzog PJ. Suppressor of cytokine signaling 1 negatively regulates Toll-like receptor signaling by mediating Mal degradation. *Nat. Immunol.* 7(2): 148-155. (2006).

11. Dey M, Cao C, Dar AC, Tamura T, Ozato K, Sicheri F, and Dever TE. Mechanistic link between PKR dimerization, autophosphorylation, and eIF2a substrate recognition. *Cell.* 122: 901-913. (2005)

12. Garcia MA, Gil J, Ventoso I, Guerra S, Domingo E, Rivas C, and Esteban M. Impact of protein kinase PKR in cell biology: from antiviral to antiproliferative action. *Microbial. Mol. Biol. Rev.* 70(4): 1032-1060. (2006)

13. Wang X, and Liu Y. Regulation of innate immune response by MAP kinase phosphatase-1. *Cell. Signal.* 19: 1372-1382. (2007)

14. Franklin CC, and Kraft AS. Conditional expression of the mitogen-activated protein kinase (MAPK) phosphatase MKP-1 preferentially inhibits p38 MAPK and stress-activated protein kinase in U937 cells. *J. Biol. Chem.* 272(27): 16917-16923. (1997)

15. Hu J-H, Chen T, Zhuang Z-H, Kong L, Yu M-C, and Liu Y. Feedback control of MKP-1 expression by p38. *Cell. Signal.* 19: 393-400. (2007)

16. Weinrauch Y, and Zychlinsky A. The induction of apoptosis by bacterial pathogens. *Annu. Rev. Microbiol.* 53: 155-187. (1999)

17. Hacker G, and Fischer SF. Bacterial anti-apoptotic activities. *FEMS Microbiol. Lett.* 211: 1-6. (2002)

18. Gao L-Y, and Kwalk YA. The modulation of host cell apoptosis by intracellular bacterial pathogens. *Trends Microbiol.* 8(7): 306-313. (2000)

19. Viboud GI, and Bliska JB. Yersinia outer proteins: role in modulation of host cell signaling responses and pathogenesis. *Annu. Rev. Microbiol.* 59: 69-89. (2005)

20. Orth K, Palmer LE, Bao Z-Q, Stewart S, Rudolph AE, Bliska JB, and Dixon JE. Inhibition of the mitogen-activated protein kinase kinase superfamily by a Yersinia effector. *Science.* 285: 1920-1923. (1999)

21. Orth K, Xu Z, Mudgett MB, Bao Z-Q, Palmer LE, Bliska JB, Mangel WF, Staskawicz B, and Dixon JE. Disruption of signaling by Yersinia effector YopJ, a ubiquitin-like protein protease. *Science.* 290: 1594-1597. (2000)

22. Park JM, Greten FR, Li Z-W, and Karin M. Macrophage apoptosis by anthrax lethal factor through p38 MAP kinase inhibition. *Science.* 297: 2048-2051. (2002)

23. Zhang Y, and Bliska JB. Role of Toll-like receptor signaling in the apoptotic response of macrophages to *Yersinia* infection. *Infect. Immun*. 71(3): 1513-1519. (2003)

24. Zhang Y, Ting AT, Marcu KB, and Bliska JB. Inhibition of MAPK and NF-kB pathways is necessary for rapid apoptosis in macrophages infected with *Yersinia*. *J. Immunol.* 174: 7939-7949. (2005)

25. Janes KA, Albeck JG, Gaudet S, Sorger PK, Lauffenburger DA, and Yaffe MB. A systems model of signaling identifies a molecular basis set for cytokine-induced apoptosis. *Science.* 310: 1646-1653. (2005)

26. Janes KA, Kelly JR, Gaudet S, Albeck JG, Sorger PK, and Lauffenburger DA. Cue-signal-response analysis of TNF-induced apoptosis by partial least squares regression of dynamic multivariate data. *J. Comput. Biol.* 11(4): 544-561. (2004)

27. Kemp ML, Wille L, Lewis CL, Nicholson LB, and Lauffenburger DA. Quantitative network signal combinations downstream of TCR activation can predict IL-2 production response. *J. Immunol.* 178: 4984-4992. (2007)

28. Miller-Jensen K, Janes KA, Brugge JS, and Lauffenburger DA. Common effector processing mediates cell-specific responses to stimuli. *Nature.* 448: 604-608. (2007)

29. Geladi P, Martens H, Hadjiiski L, and Hopke P. A calibration tutorial for spectral data. Part 2. Partial least squares regression using Matlab and some neural network. *J. Near Infrared Spectrosc.* 4: 243-255. (1996)

30. Umetrics AB. User's guide to SIMCA-P, SIMCA-P+ Version 11.0. (2005)

31. Geladi P, and Martens H. A calibration tutorial for spectral data. Part 1. Data pretreatment and principal component regression using Matlab. *J. Near Infrared Spectrosc.* 4: 243-255. (1996)

32. Stone AA, and Chambers TC. Microtubule inhibitors elicit differential effects on MAP kinase (JNK, ERK and p38) signaling pathways in human KB-3 carcinoma cells. *Exp. Cell Res.* 254: 110-119. (2000)

33. Jarvis WD, Fornari FA, Auer KL, Freemerman AJ, Szabo E, Birrer MJ, Johnson CR, Barbour SE, Dent P, and Grant S. Coordinate regulation of stress- and mitogen-activated protein kinases in the apoptotic actions of ceramide and sphingosine. Mol. Pharmacol. 52: 935-947. (1997)

34. Medzhitov R, Preston-Hurlburt P, and Janeway CA Jr. A human homologue of the Drosophila Toll protein signals activation of adaptive immunity. Nature. 388: 394-397. (1997)

Figure 1

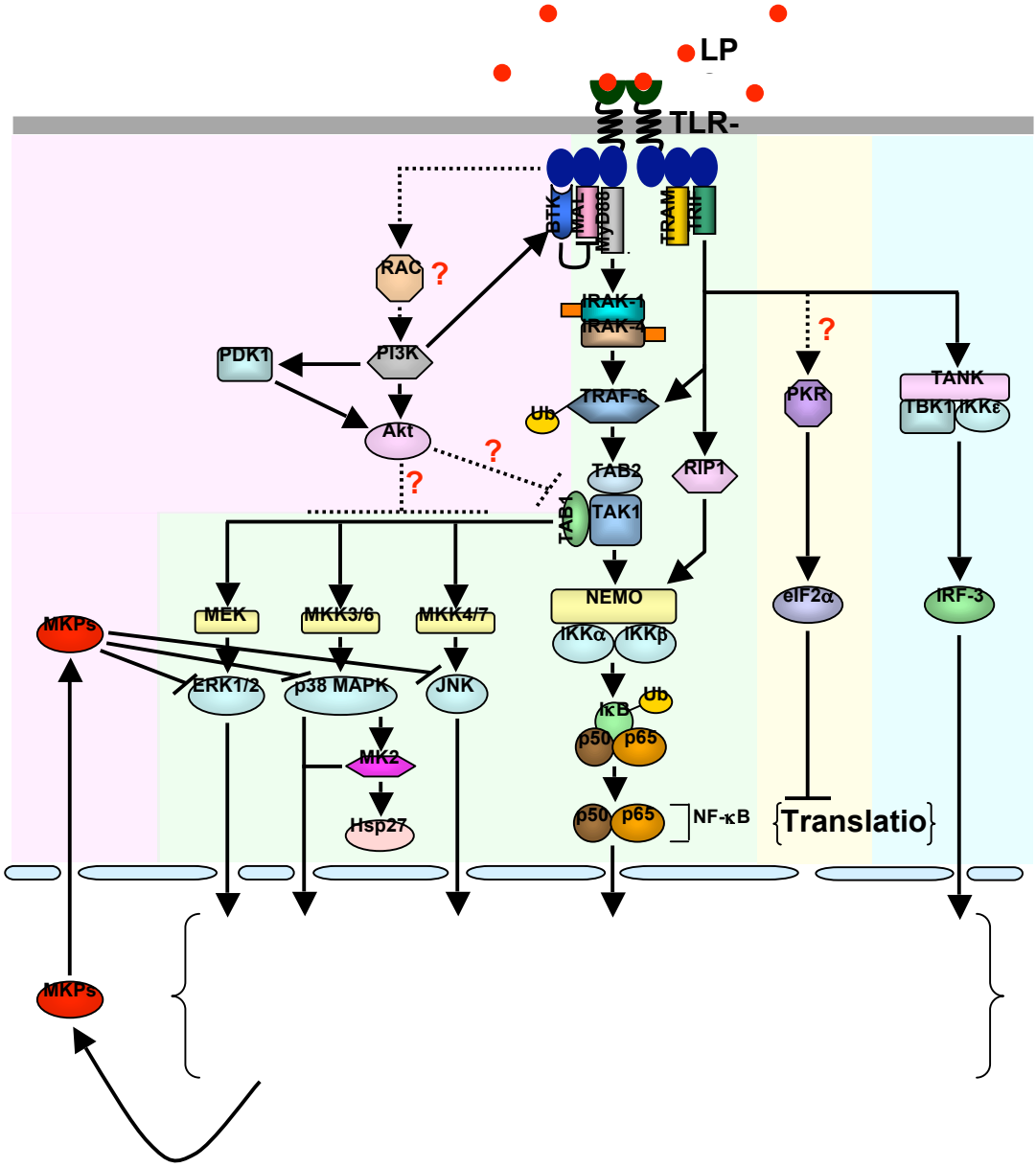

Figure 2

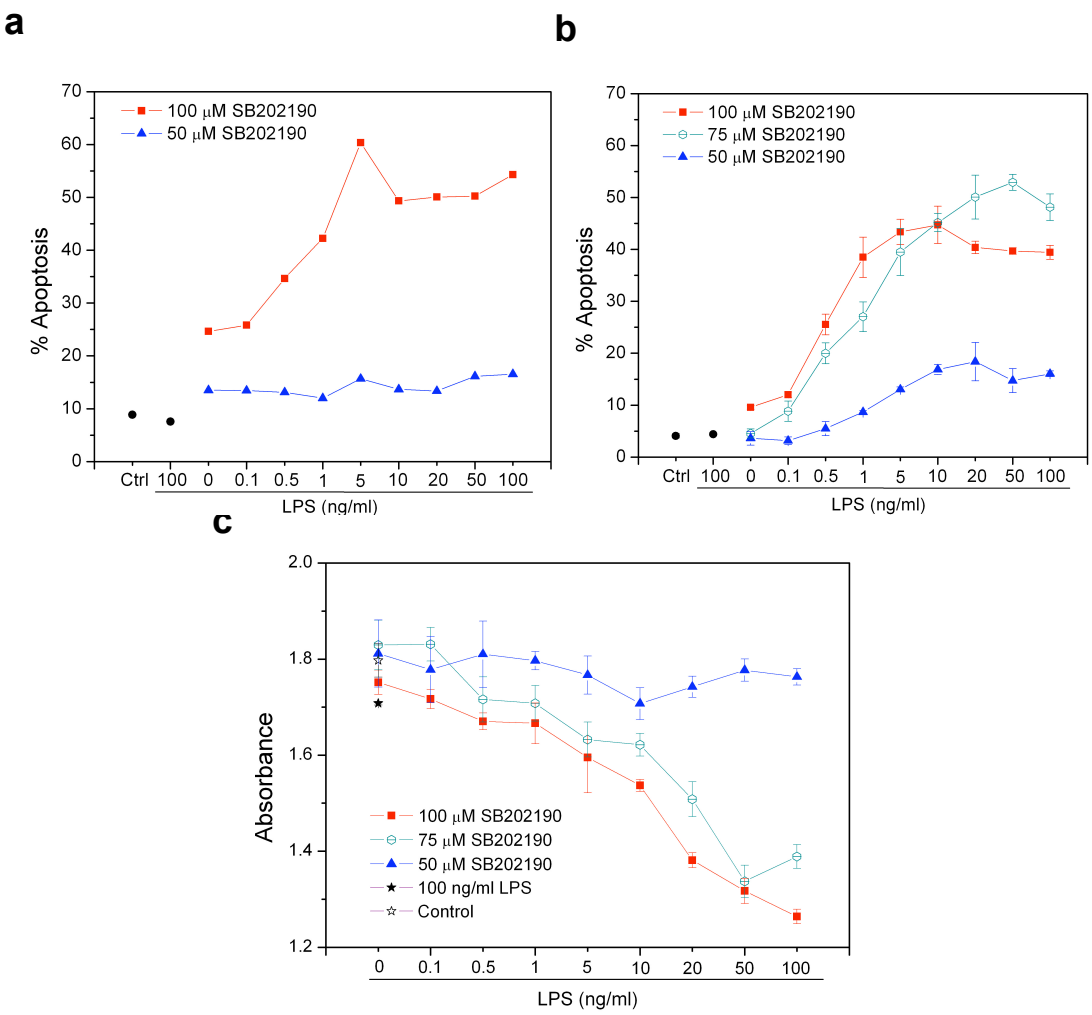

Figure 3a

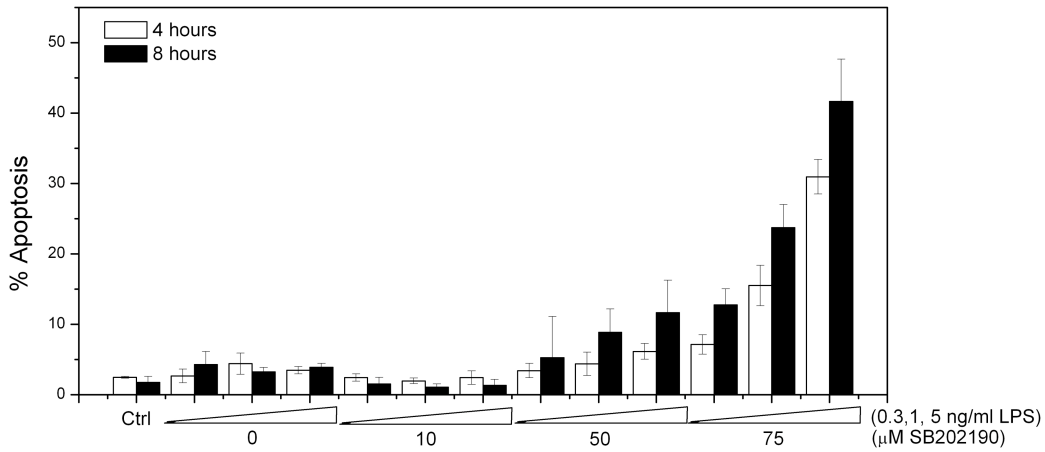

Figure 3b

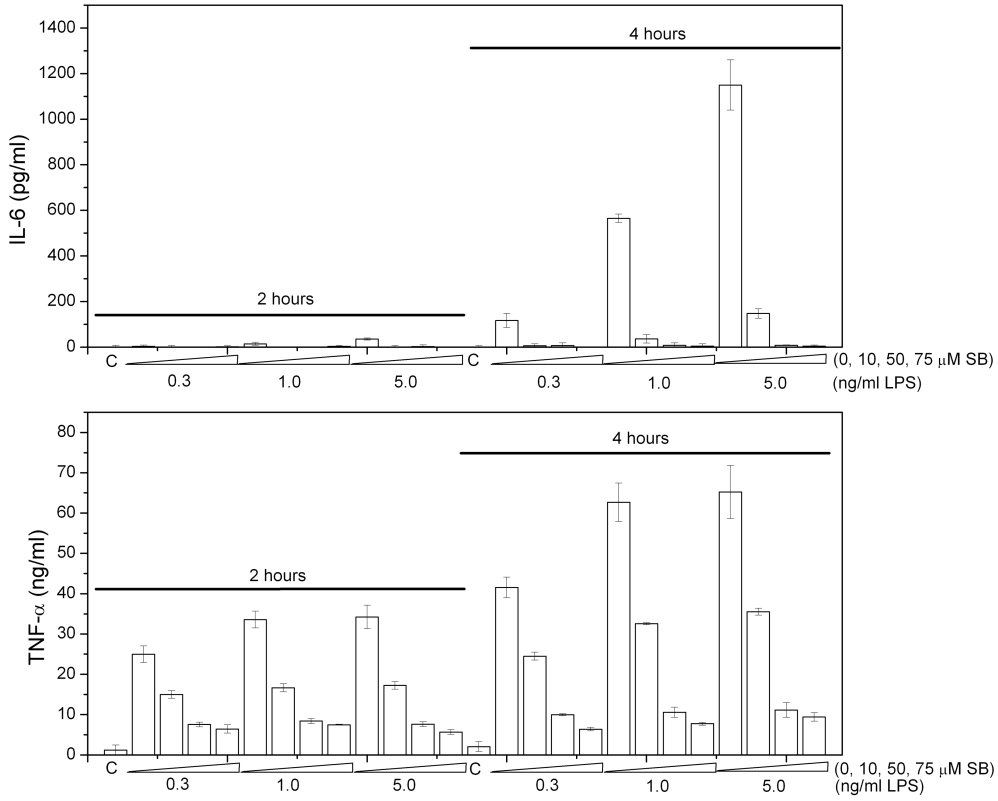

Figure 4

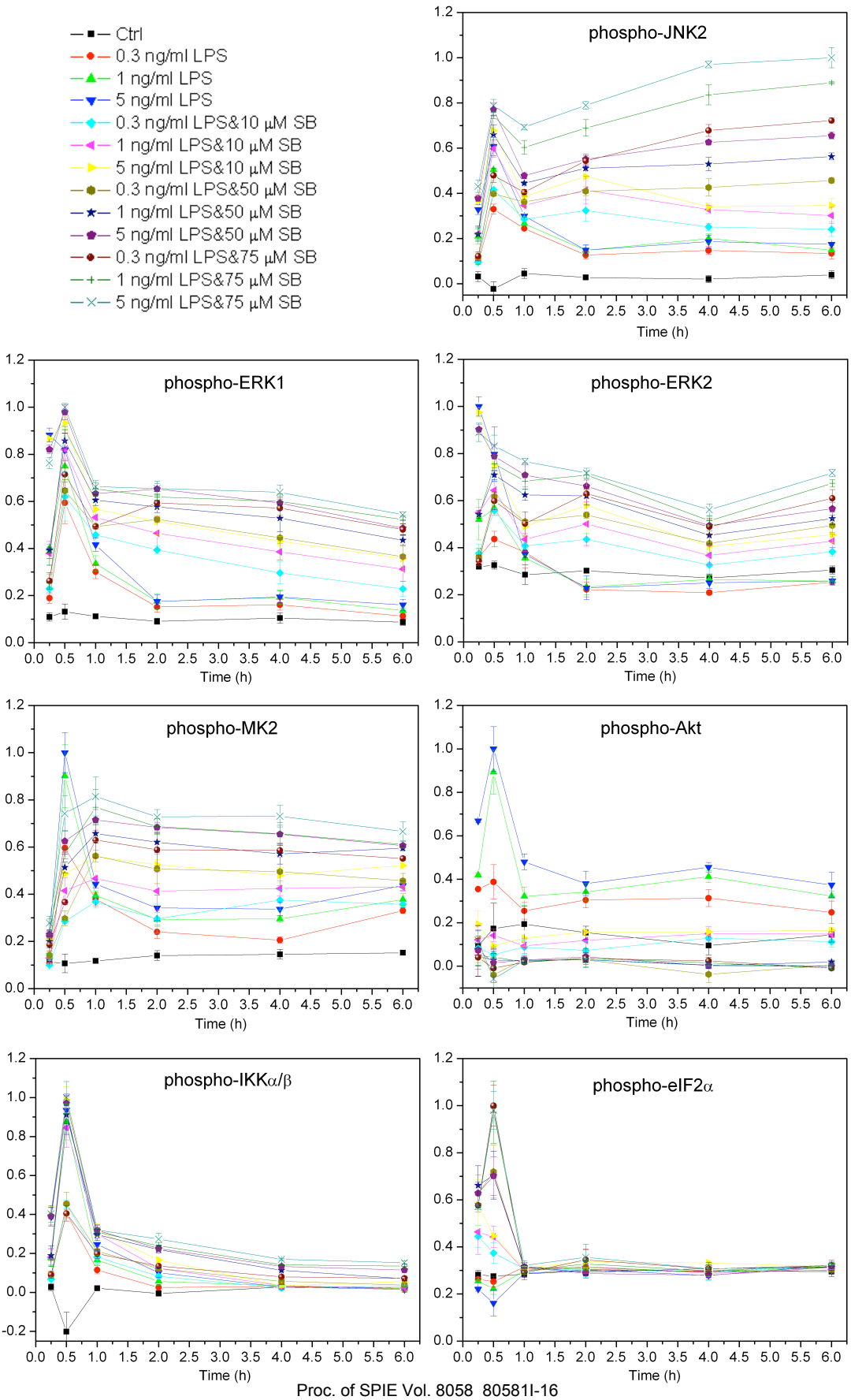

Figure 5

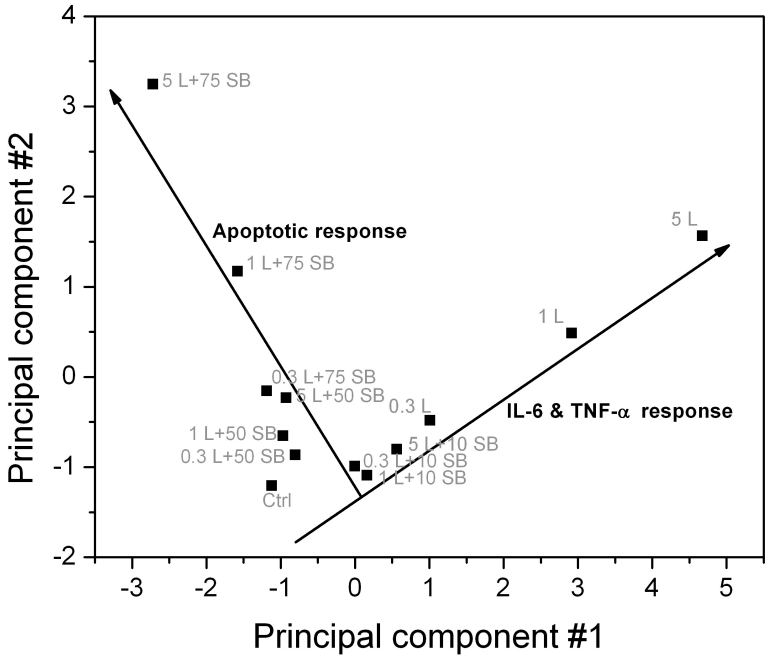

Figure 6

a

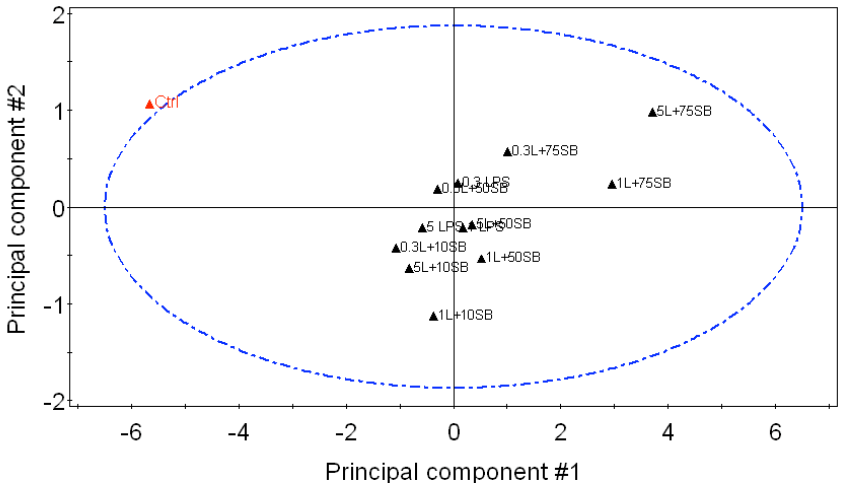

b

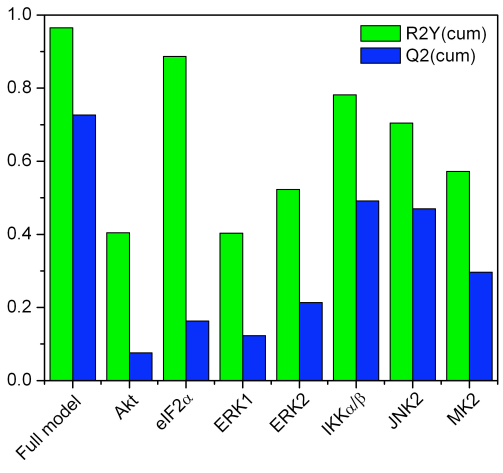

c

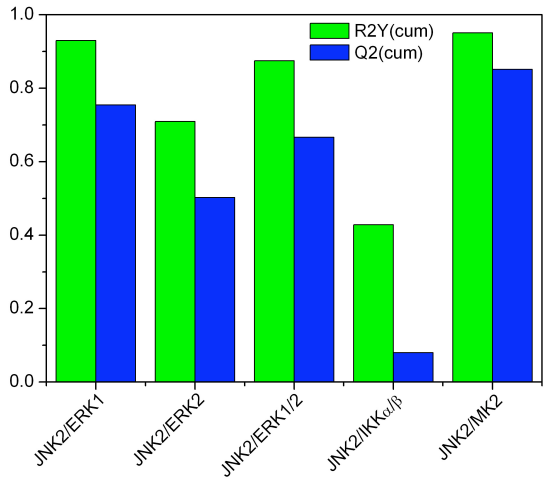

Figure 7

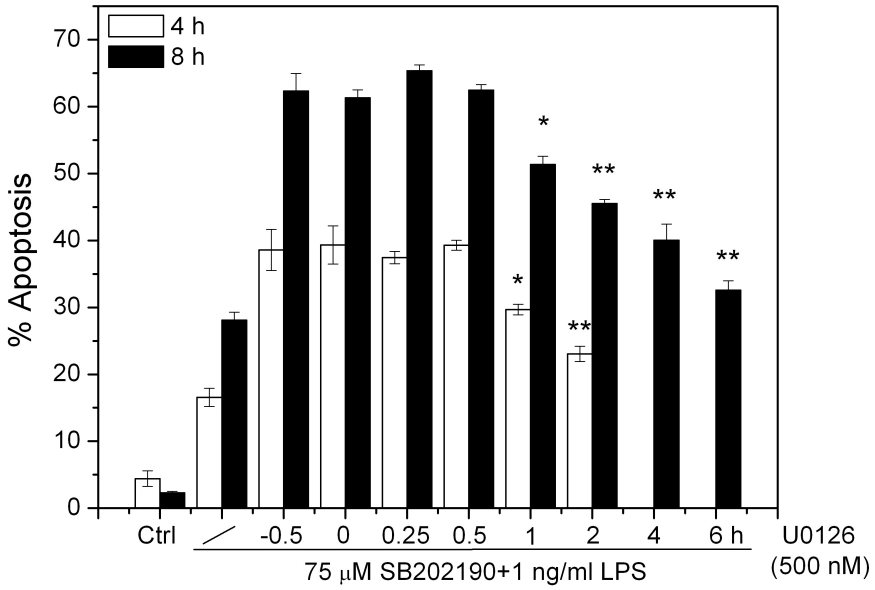

Figure 8